

**ERUPTIVE PROCESSES IN THE AVERNO 2 ERUPTION  
(CAMPI FLEGREI - ITALY): CONSTRAINTS BY PHYSICAL  
PROPERTIES OF THE JUVENILE FRAGMENTS**

CÉLINE FOURMENTRAUX

Dipartimento di Scienze della Terra, Università di Pisa, Via S. Maria 53, 56126 Pisa

ABSTRACT

The Averno 2 eruption (Av2) occurred 3.7 ka b.p in the northwest sector of the Campi Flegrei caldera (CFc), at the intersection of NE-SW and NW-SE fault systems bordering the resurgent block. The eruption, one of the youngest of the caldera, was followed only by the 1538 AD eruption of Monte Nuovo. 21 representative samples of Av2 deposits were analyzed for grain-size and componentry whereas 16 depositional units (about 100 juvenile clasts each) were sampled to measure bulk density, bulk vesicularity and assess texture characteristics of individual clasts. According to bulk density, vesicularity and textural data, three main pyroclasts types were identified: i) low-density, light coloured, microvesicular, microlite-free; ii) high-density, dark-brown, microlite-rich; iii) banded made up to mm-thick stripes of (i) and (ii) types. The three types record variations of magma properties resulting from various degassing histories and syn-eruptive crystallization of groundmass. Characteristics and relative abundance of juvenile clast types throughout the stratigraphic sequence were used to make inferences and place constrains on temporal variations in magma rise and eruptive mechanisms. Occurrence in the very early fallout bed of dense juvenile clasts suggests the initial disruption of a limited volume of degassed magma. Member A was dominated by type (i) clasts suggesting that plinian episodes were fed by the fast supply of volatile-rich highly evolved magma from below whereas subsequent eruptions were fed by volatile poor-magma less evolved (member C). Members B and C contain (i), (ii), and (iii) types and increasing abundance throughout time of clasts (ii) and (iii) suggests increasing importance of intra-eruption degassing, mostly occurring during time breaks between two successive eruptive pulses. The pulsating activity of Av2 appears to be transitional in style between subplinian and vulcanian and we propose that transitions in eruptive style from plinian to surge activity were controlled by magmatic processes and not by water-magma interaction.

INTRODUCTION

Recent activity in the CFc has been dominated by explosive eruptions of variable magnitude that generated alternating fallout beds and pyroclastic-surge deposits (*e.g.*, Barberi *et al.*, 1988, Wohletz *et al.*, 1995; De Vita *et al.*, 1999; Dellino *et al.*, 2001, 2004). Several authors have emphasized that the explosivity of most events requires in part, the exsolution of magmatic volatiles (formation of pumice) and, in part, the interaction of magma with water (formation of wet, accretionary lapilli-rich, ash deposits). Starting from this concept, several authors have also attempted to discriminate magmatic versus hydromagmatic phases on the basis of different criteria. Some have considered base surge deposits to have been generated by magma-water interaction; others have used clast morphological features (ash grains) to discriminate between different mechanisms of magma fragmentation (Wohletz, 1983; Cioni *et al.*, 1992; Büttner *et al.*, 1999, 2002). However, several studies have suggested that variations in explosive

eruptive style can be explained by changes in magma properties due to groundmass crystallization and corresponding changes in magma rheology. Indeed, recent textural studies of volcanic products from historical Campi Flegrei eruptions (*e.g.*, D’Oriano *et al.*, 2005; Mastrolorenzo *et al.*, 2006) provide evidence that degassing and crystallisation during magma ascent could strongly influence the style and evolution of the eruption. Syn-eruptive degassing/crystallisation has been shown to be a very effective process in controlling Vulcanian style eruptions of calc-alkaline composition. Recent examples include Mount St. Helens (USA) in 1980 (Cashman & Mc Connell, 2005), Galeras (Colombia) in 1992 (Stix *et al.*, 1997; Cruz & Chouet, 1997), Souffrière Hills (Montserrat) between 1995 and 1999 (Druitt & Kokelaar, 2002; Formenti *et al.*, 2003), Guagua Pichincha (Ecuador) in 1999 (Wright *et al.*, 2007).

The Av2, dated at 3700 years BP (Alessio *et al.*, 1971), is one of the youngest and best preserved volcanic structures of the CFc (Fig. 1). Av2 represented a moderate-magnitude event in the volcanic history of CFc and was characterized by complex eruptive activity with alternating plinian to surge



Fig. 1 - View of Averno lake.

activity that generated a sequence of pyroclastic-fall and -ash deposits. According to Di Vito *et al.* (2001) and Braia (2003) deposits are subdivided in three members named A, B, and C (Fig. 2). The lower member A (Fig. 2a and 2b) consists of 6 pumice fallout beds intercalated to thin ash and lapilli beds (surge). The upper members (B and C) are mainly dominated by dry surges beds and minor wet surges (Fig. 2c and 2d). Previous workers have concluded that the explosive activity evolved from prevalent magmatic (member A) to pure hydromagmatic style (members B and C). Thus, the eruption of Av2 provides an ideal case to investigate possible differences between juvenile clasts of varying eruptive dynamics with the aim of better documenting the actual role of magmatic explosivity and its evolution with time. Our research is carried out in order to investigate the responsible mechanisms for the evolution in eruptive style that generated this complex pyroclastic sequence. Here, we present data on the physical properties (bulk density, bulk vesicularity, and macro and micro-texture) of the juvenile clasts. The Av2 eruption represents a possible scenario expected in this sector of the caldera, in case of a future eruption. Therefore, this subject represents a fertile area of research since it improves our knowledge of the CFc eruptions and may be important in terms of volcanic hazard assessment and risk management at CFc.

## RESULTS

### *Macroscopic texture of the juvenile clasts*

Pumice clasts from the fallout and surge deposit are heterogeneous and show a large variability in morphology and texture. Clasts are distinct in their colours and differ in density, vesicle content, size,

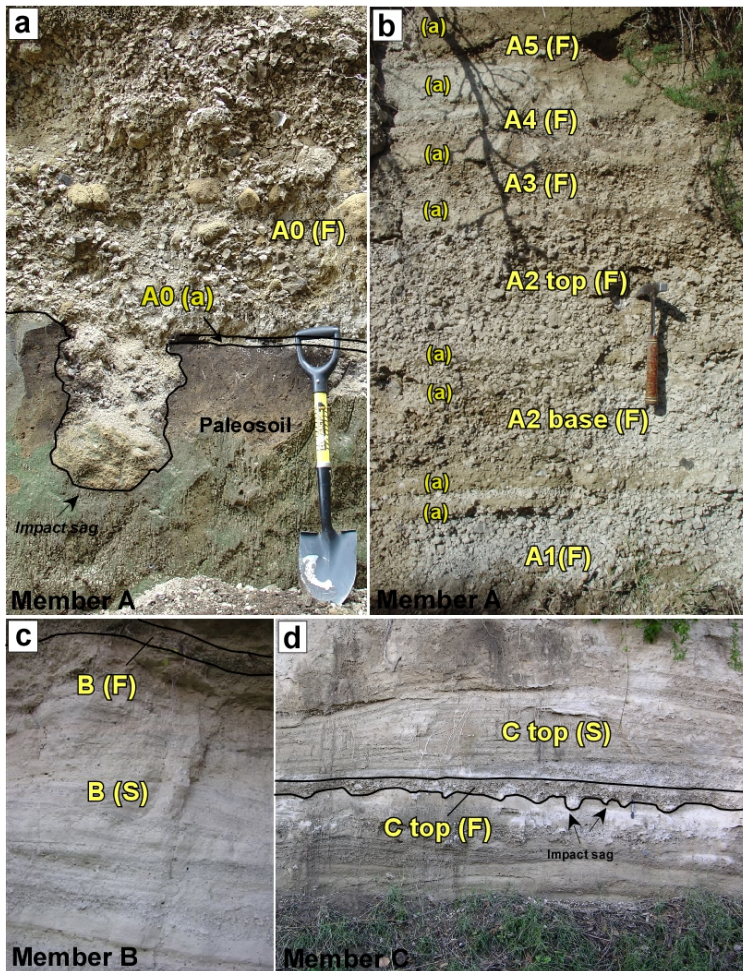


Fig. 2 - (a) Member A fallout bed A0(a) associated with coarse grained A0(F) fallout bed; (b) fallout deposits from A1(F) to A5(F) intercalated to minor ash-surge beds (a); (c-d) Member B and member C respectively, dominated by surge sequence (S) with subordinate fallout beds (F).

shape and spatial distribution. As a result, three morphological clast types are distinguished: light-coloured clasts, banded, and dark-brown coloured clasts (Fig. 3).

i) Light-coloured clasts are microvesicular pumice displaying both isotropic (Fig. 3a) and tubular (Fig. 3b) textures. They are extremely to moderately vesicular, containing vesicles that vary in shape (from tubular to contorted or spherical) and dimension.

ii) Dark brown clasts are, in general, angular and either non-vesicular or very poorly-vesicular, dense with superficial fractures. Some blocks contain angular lithic fragments which can be interpreted as the incorporation of the walls of the conduit during the ascent of the magma in a high shear environment (Fig. 3d).

iii) Banded clasts cover a wide range of morphological features from highly vesicular to poorly vesicular, and are characterized by an alternation of white/yellow and dark or pale grey/brown bands (Fig. 3c). A few banded bomb exhibit breadcrusted forms typical of vulcanian eruptions. Included in this category are clasts with alternating non-vesicular dark-brown coloured and obsidian texture bands (Fig. 3c).

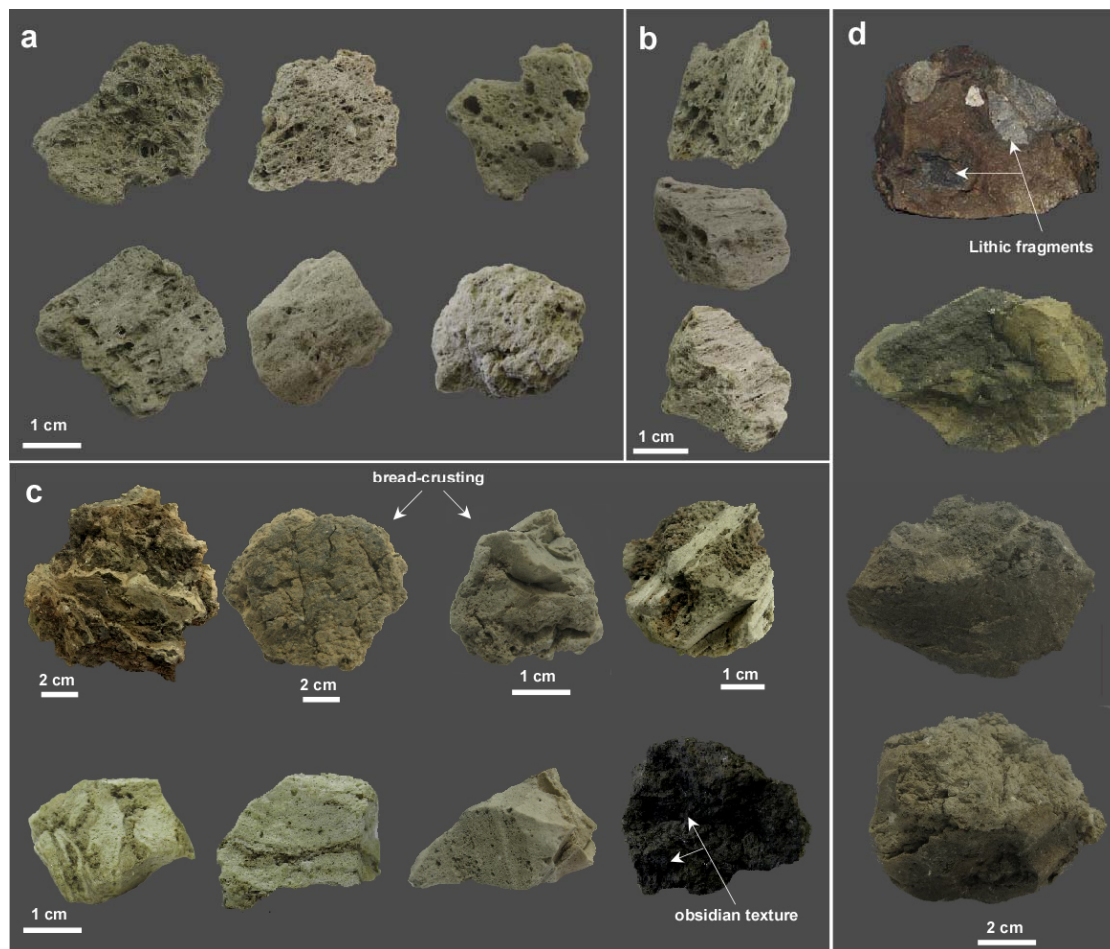


Fig. 3 - Examples of Juvenile products from Averno 2 eruption. General view of: (a) light-coloured clasts with isotropic texture; (b) light-coloured clasts with tubular texture; (c) banded pumice with obsidian-like texture and clasts showing bread-crusting; (d) dark-brown coloured types. (c) and (d) show bread-crusting.

*Clast density and vesicularity*

Density was measured on 1589 clasts taken from 15 layers sampled through the entire stratigraphic sequence (Table 1). In each member, clasts of fallout and surge deposits show a wide variation in density of juvenile clasts ranging from 300 to 2500 kg/m<sup>3</sup> and corresponding to a vesicularity range of 89-8% (Table 1). According to the classification scheme proposed by Houghton & Wilson (1989), clasts range from extremely to poorly-vesicular. To provide a full description of the evolution of parameters during the Averno 2 eruption, we introduced in the density histograms the three morphological clasts type identified (Fig. 4 and 5). It can be immediately observed that, the variation of densities observed in fallout and surge deposits reflects variations in clast types. Microvesicular clasts have the lowest density (530 to 660 kg/m<sup>3</sup>), while dark brown clasts have the highest density (1660-1820 kg/m<sup>3</sup>). Banded clasts are intermediate with the widest density range from 500 to 1130 kg/m<sup>3</sup>. All samples of the member A, except the two lowermost ones A0 and A1, have an uniform density (Table 1 and Fig. 4). In details, the fallout beds of member A are characterized by an unimodal distribution containing uniform pumice assemblage

Table 1 - Average of bulk rock density and vesicularity of Averno 2 juvenile components; n: number of clasts;  $\rho$ : density;  $\sigma$ : standard deviation; the second number in the label indicate the number of the outcrop.

Sample	Deposit	Member	n	Average $\rho$ ( $10^3 \text{ kg m}^{-3}$ )	$\sigma$ ( $10^3 \text{ kg m}^{-3}$ )	$\rho$ range ( $10^3 \text{ kg m}^{-3}$ )	Vesicularity (% vol)	$\sigma$ (% vol)	Vesicularity range (% vol)
A0- (1)	Fallout	A	100	0.61	0.23	0.3-1.5	77.4	8.7	46.5-89.6
A1- (2)	Fallout	A	100	0.49	0.09	0.4-0.8	81.8	3.2	71.3-88.2
A2 b- (2)	Fallout	A	100	0.57	0.17	0.4-1.5	79.1	6.2	45.7-88.2
A2 t- (2)	Fallout	A	100	0.53	0.12	0.4-0.9	80.6	4.3	67.4-87.6
A3- (2)	Fallout	A	100	0.53	0.12	0.4-1.1	80.5	4.5	58.3-88.5
A4- (2)	Surge	B	102	0.73	0.36	0.4-1.9	73.1	13.3	32.9-88.5
B b- (3)	Fallout	A	100	0.57	0.19	0.4-1.5	79.1	7.1	44.9-87.6
B t- (4)	Fallout	C	99	0.67	0.26	0.4-1.5	75.4	9.4	47.1-88.8
C mb- (5)	Surge	C	119	0.89	0.33	0.4-2.0	67.2	12.2	26.4-85.5
C mb- (7)	Fallout	C	100	0.72	0.26	0.4-1.7	73.4	9.7	39.7-87.7
C t- (5)	Surge	C	109	0.86	0.37	0.4-2.5	68.3	13.5	10.9-85.7
C t- (5)	Surge	C	120	0.56	0.19	0.4-1.9	80.3	5.7	30.8-90.1
C t- (6)	Surge	C	120	0.61	0.20	0.4-1.5	77.6	7.2	46.1-87.5
C mb-s1 (5)	Surge	C	120	0.86	0.37	0.4-2.1	68.3	13.6	23.6-87.6
C mb-s2 (5)	Fallout	C	100	0.75	0.38	0.4-1.9	72.5	13.4	32.3-87.6
C mb-s3 (5)	Fallout	C	109	0.88	0.36	0.4-1.9	67.6	14.0	29.9-85.3

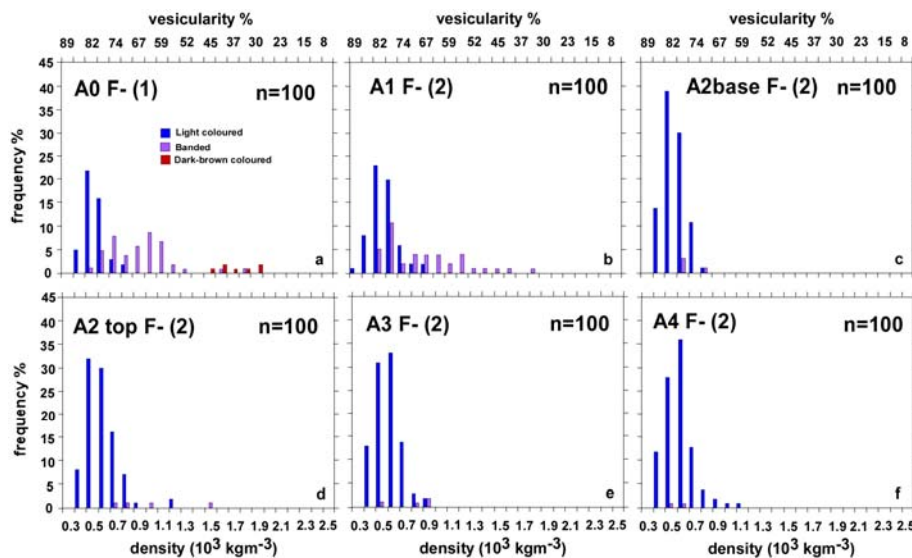


Fig. 4 - (a-f) Density/vesicularity distribution of Averno 2 pyroclasts from each fallout deposit of member A. Excluding A0 F and A1 F, deposits contain uniform pumice assemblages, with a single sharp peak of density and vesicularity of  $500 \text{ kg m}^{-3}$  and 82% respectively. Letters denote: F, fallout; n, number of analysed clasts. Vesicularity values are derived using a measured DRE value of  $2714 \text{ kg m}^{-3}$ .

with a single, sharp peak between  $500$  and  $600 \text{ kg/m}^3$  corresponding to a vesicularity range of 82-78%. A0 and A1 fallout are clearly heterogeneous layers exhibiting the widest range in density from  $400$  to  $1900 \text{ kg/m}^3$  and  $300$  to  $1500 \text{ kg/m}^3$  respectively. Density of fallout and surge deposits in member B range

from 400 to 1900 kg/m<sup>3</sup> and reflect the large variability of banded clast (Fig. 5a-b). Density distributions of analysed samples of member C from both fallout and surge deposits are bimodal (Fig. 5c-f). Densities

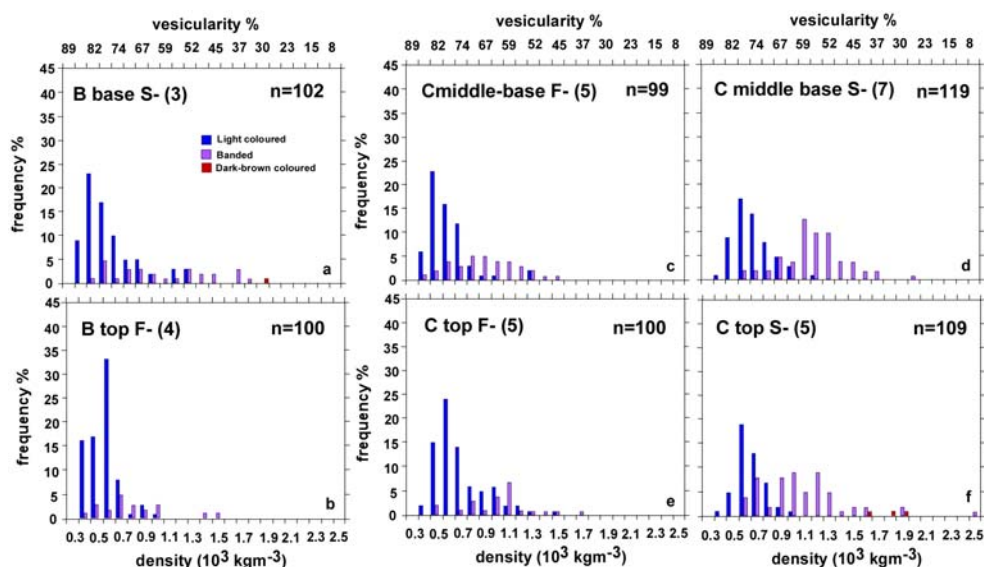


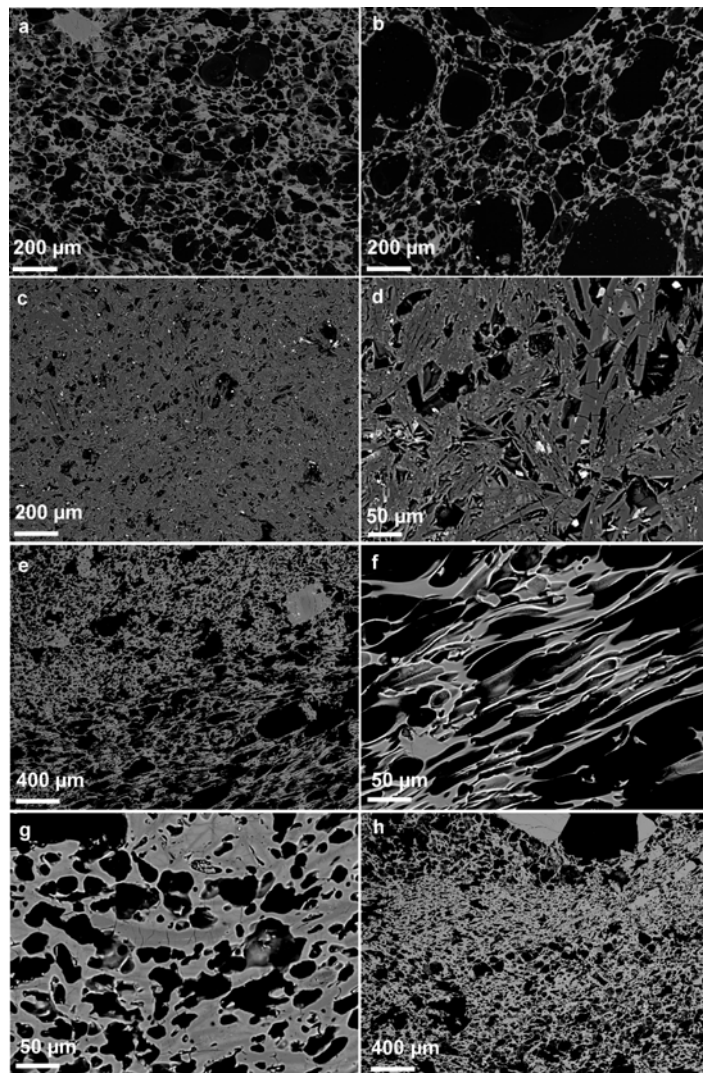
Fig. 5 - (a-b) Density/vesicularity distribution of Averno 2 pyroclasts from fallout and surge deposits of member B. (c-g) Density/vesicularity distribution of Averno 2 pyroclasts from fallout and surge deposits of member C. Letters denote: F, fallout; S, surge; n, number of analysed clasts. Vesicularity values are derived using a measured DRE value of 2714 kg m<sup>-3</sup>.

cover a wide range from 400 to 2500 kg/m<sup>3</sup>. The density shifts from the base (400-1500 kg/m<sup>3</sup>) in Cmb-(5) to (400-2500 kg/m<sup>3</sup>) in Ct-(5) (Fig. 5). We note that each deposit contains highly vesicular clasts showing peaks at minimum densities 500-600 kg/m<sup>3</sup>. The overall deposits of member C are more heterogeneous exhibiting an apparent secondary peak toward to highest densities from 1,000 kg/m<sup>3</sup> to 1,400 kg/m<sup>3</sup> which correspond to a vesicularity range of 63-48%. Clast density/vesicularity data highlights the contrast between member A, B and C. Each heterogeneous sample through the stratigraphic sequence probably represents a mixture of a highly vesiculated magma and partially degassed magma which formed during time breaks at shallow depth.

*Microscopic texture of the juvenile clasts*

To determine the relationship between density and groundmass crystallinity, we examined thin sections of representative juvenile clasts using both optical microscopy and SEM. Indeed, a positive correlation between microlite crystallization and density and negative correlation with vesicularity is related to variations in rates of magma ascent. This correlation can be directly attributed to the times available for gas loss (Jaupart, 1998) and degassing-induced crystallization (e.g., Hammer *et al.*, 1999). BSE images taken at low magnification offer a general view of each clast types (Fig. 6). On the basis of pyroclasts density and groundmass texture, we have identified the three different pyroclasts types described above. (i) Light coloured, microvesicular clasts which have a low density ( $\rho$ ) ( $\rho < 900 \text{ kg/m}^3$ ) are highly vesicular and found in all deposits. They can exhibit subspherical vesicles whose diameter is

Fig. 6 - Backscattered electron (BSE) images of representative pyroclast types. a-b light-coloured, microvesicular pumice; scale bar = 200  $\mu\text{m}$ ; c-d dark brown-coloured clast; scale bars = 200  $\mu\text{m}$  and 50  $\mu\text{m}$ , respectively; e banded pumice clasts of member A; scale bar = 400  $\mu\text{m}$ ; f white band in banded pumice clasts of member A; scale bar = 50  $\mu\text{m}$ ; g brown dark band in banded pumice clasts of member A, scale bar = 50  $\mu\text{m}$ ; h banded pumice clast of member C; scale bar = 400  $\mu\text{m}$ . Black irregular shapes are vesicles, grey background is glass, grey crystals are plagioclase and sanidine, white crystals are oxide phases.



generally less than 50  $\mu\text{m}$  in diameter (Fig. 6a) or larger deformed vesicles with a large diameter (up to one millimeter) associated with smaller vesicles which tend to be subspherical in a glassy groundmass (Fig. 6b). Highly elongated and stretched vesicles aligned into a preferred direction are exhibited by tube pumice clasts (Fig. 6f). (ii) Dark brown coloured clasts with the highest density (1500-2100  $\text{kg}/\text{m}^3$ ) have a vesicularity which decreases in terms of both vesicle abundance and dimension (Fig. 6c). These clasts have a holocrystalline texture containing microphenocrysts (up to 250  $\mu\text{m}$ ) either as isolated or as clusters (Fig. 6d). (iii) Banded clasts exhibit a wide range of densities ( $\rho = 400\text{-}2000 \text{ kg}/\text{m}^3$ ) reflecting the wide range of morphological features of these clasts. They have a vesicularity and groundmass crystallinity which are organised in bands (Fig. 6e, 6h). The light bands have a heterogeneous vesicularity, with large vesicles from elongated (Fig. 6f) to large or small subspherical whereas in dark bands have large deformed vesicles associated with small spherical vesicles (Fig. 6g). Banded clasts show a range of clasts densities that reflects a variably crystallised groundmass, band with light coloured groundmass exhibit the absence (Fig. 6f) or some microlite while band dark colour are always microlite-rich (Fig. 6g). The banded clasts with obsidian have the highest density ( $\rho = 2500 \text{ kg}/\text{m}^3$ ). Examination of pyroclastic

obsidian microtexture reveals the alternation of dark brown and glassy bands with spherulitic texture. The obsidian bands have large deformed and elongated vesicles and contain some microlites. The dark-brown bands have a holocrystalline groundmass textures with irregular vesicles (50-100  $\mu\text{m}$ ).

## DISCUSSION

Using, bulk density, vesicularity and textural data, three main pyroclast types were identified: i) low-density, light coloured, microvesicular, microlite-free clasts; ii) high-density, dark-brown, microlite-rich clasts; iii) banded clasts made up of mm-thick stripes of (i) and (ii) types. The light-coloured microvesicular pumices (heterogeneous vesicles and elongated/deformed vesicles) are typical product of magmatic explosive eruptions. The origin of pumice clasts with different textural and morphological characteristics is attributed in the literature to the development of conduit regions marked by different rheological behaviour (see Cashman *et al.*, 2000; Polacci *et al.*, 2001, 2003). The central part of the conduit is occupied by microvesicular pumice clasts whereas tube-shape pumices are suggested to originate in the region between the center and the conduit walls by both high strain rates in response to shearing at the conduit walls and elongational strain during magma ascent (Sparks *et al.*, 1994; Cashman *et al.*, 2000; Polacci *et al.*, 2001, 2003). Microlite textures are correlated with volatile-loss. Dark-brown coloured clasts are microlite rich and have the lowest vesicularity suggesting that degassing during ascent causes the magma to crystallize. This deduce this with comparison other eruption where occurs the same process (*e.g.*, Cashman *et al.*, 2000, 2005; Hammer *et al.*, 1999). In addition, the occurrence in the deposits of both dark-brown microlite-rich clasts containing foreign lithic fragments inside and obsidian-bearing material suggests that they probably derived from dikes or wall rock fractures filled with “vanguard” magma that, together with wall rocks, were eroded and incorporated into (Rust & Cashman, 2007). We also suggest that banded clast were be formed by pure syn-eruptive mingling of deeper magma with “vanguard” magma that was involved in creating dike fractures and that stalled temporarily at intermediate levels. Also, we propose that the story of Averno 2 eruption can be modelled as follow. During the first phase (member A), the magma that crystallized in response to the degassing was pressurized by new faster-rising magma from depth in the interior part of the conduit, expelled and mingled with the dense and viscous plug producing a heterogeneous fallout bed with a limited amount of dense juvenile clasts (A0 fallout breccia). After this opening stage, 6 fallout beds (from A1(F) to A5 (F)) intercalated by thin ash layers were deposited by pulsatory sub-plinian eruptions with a variable eruptive columns (between 4-10 km high; estimate by Di Vito *et al.*, 2001). This stage was dominated by type (i) clasts (light microvesicular, isotropic and tubular texture) suggesting that, the pulsatory sub-plinian episodes were fed by the fast supply of volatile-rich magma from below. In contrast, the occurrence and increase in abundance of types (ii) and (iii) in the upper unit (member C), suggests the increasing importance of intra eruption degassing, mostly occurring during time breaks between successive eruptive pulses. For each discrete eruptive pulse the progressive decline of the magma supply rate (MSR) and both the reduced pre-eruptive volatile content and the deepening of the fragmentation front (reducing the exit velocity of the gas/pyroclats mixture) favoured the collapse of the eruptive fountain. Intra-pulse degassing was likely responsible for the emplacement of dry to accretionary-lapilli bearing, fine-ash fall out beds separating the surge bedset. The sample from member B represents the transition between the two extremes A and C. Thus, we propose that transitions in eruptive style from plinian to surge activity are the consequence of an eruption controlled by magmatic processes in which each discrete eruptive pulse was fed by the propagation downward of the fragmentation front. Increasing separation between successive

pulses is likely the consequence of a decline of magma supply rate from below. Reduced exit velocities during surge emplacements of B and C members are probably accounted by reduction of magmatic pre-eruptive volatile content and change in magma properties due to degassing and to groundmass crystallization and corresponding changes in magma rheology. Data on juvenile clasts support that fragmentation was dominated by purely magmatic processes, magma-water interaction if present, exerted a subsidiary role in the magma fragmentation and emplacement of surges.

## CONCLUSION

The Averno-2 eruption shows a change in eruptive regime through time from dominantly sustained (sub-plinian) to dominantly pulsating (surge). Here, we have shown that data on the physical characteristics (density, vesicularity and macro and micro-texture) of the juvenile clasts are fully accounted by an eruptive mechanism regulated by the interplay of magma supply rate, syn-eruptive degassing and microlite crystallization of magma in the conduit. The implications of this conclusion are many. Firstly, it provides an explanation for producing dense juvenile clasts without calling on interaction with external water. Secondly, it suggests that microlite in these pyroclasts preserve a detailed record of variations in magma ascent and degassing rates throughout the eruptive sequence. Lastly it requires temporary storage of magma at shallow levels before each eruptive pulse. Our interpretation accounts for the occurrence of the juveniles with contrasting densities and texture in the deposits and the increasing abundance through time of dense juvenile (ii) and (iii) types. Although the eruption consisted of a large number of discrete explosive pulses it is likely that the entire eruption occurred within a short period of time (hours to days). In contrast with previous interpretations, our data on the physical nature of the magmatic component also indicates that important involvement of external water is not required to account for the magma fragmentation and eruptive dynamics.

## REFERENCES

- Alessio, M., Bella, F., Improta, F., Belluomini, G., Cortesi, C., Turi, F. (1971): University of Rome C-14 dates IX. *Radiocarbon*, **13**, 395-411.
- Barberi, F., Navarro, M., Rosi, M., Santacroce, R. (1988): Explosive interaction of magma with ground water: insights from xenoliths and geothermal drillings. *Rend. Soc. It. Mineral. Petrol.*, **43**, 901-926.
- Braia, G. (2003): Metodologie quantitative per la ricostruzione dei meccanismi eruttivi di eruzioni esplosive: il caso di Averno 2 nella caldera dei Campi Flegrei. Ph.D. tesi, Università di Bari.
- Büttner, R., Dellino, P., Zimanowski, B. (1999): Identifying magma-water interaction from the surface features of ash particles. *Nature*, **401**, 688-690.
- Büttner, R., Dellino, P., La Volpe, L., Lorenz, V., Zimanowski, B. (2002): Thermohydraulic explosions in phreatomagmatic eruptions as evidenced by the comparison between pyroclasts and products from Molten Fuel Coolant Interaction experiments. *J. Geophys. Res.*, **107**, 1-13.
- Cashman, K.V. & Blundy, J. (2000): Degassing and crystallization of ascending andesite and dacite. *Phil. Trans. R. Soc.*, **358**, 1487-1513.
- Cashman, K.V. & Mc Connell, S.M. (2005): Multiple levels of magma storage during the 1980 summer eruptions of Mount St. Helens, WA. *Bull. Volcanol.*, **68**, 57-75.
- Cioni, R., Sbrana, A., Vecchi, R. (1992): Morphologic features of juvenile pyroclasts from magmatic and phreatomagmatic deposits of Vesuvius. *J. Volcanol. Geotherm. Res.*, **51**, 61-67.
- Cruz, F.C. & Chouet, B.A. (1997): Long-period events, the most characteristic seismicity accompanying the emplacement and extrusion of a lava dome in Galeras Volcano, Colombia, in 1991. *J. Volcanol. Geotherm. Res.*, **77**, 121-158.

- Dellino, P., Isaia, R., La Volpe, L., Orsi, G. (2001): Statistical analysis of textural data from complex pyroclastic sequences: implications for fragmentation processes of the Agnano-Monte Spina tephra (4.1 ka), Campi Flegrei, southern Italy. *Bull. Volcanol.*, **63**, 443-461.
- Dellino, P., Isaia, R., La Volpe, L. (2004): Interaction between particles transported by fallout and surge in the deposits of the Agnano-Monte Spina eruption (Campi Flegrei, Southern Italy). *J. Volcanol. Geotherm. Res.*, **133**, 193-210.
- De Vita, S., Orsi, G., Civetta, L., Carandente, A., D'Antonio, M., Di Cesare, T., Di Vito, M., Fisher, R.V., Isaia, R., Marotta, E., Ort, M., Pappalardo, L., Piochi, M., Southon, J. (1999): The Agnano-Monte Spina eruption (4.1 ka) in the resurgent, nested Campi Flegrei caldera (Italy). *J. Volcanol. Geotherm. Res.*, **91**, 269-301.
- Di Vito, M.A., Braia, G., Isaia, R., Orsi, G., Piermattei, M. (2001): The Averno2 eruption in the northwestern sector of Campi Flegrei caldera (Italy). GNV - Framework Program 2000/2002 - Project n. 26, 101-106.
- D'Oriano, C., Poggianti, E., Bertagnini, A., Cioni, R., Landi, P., Polacci, M., Rosi, M. (2005): Changes in eruptive style during the A.D. 1538 Monte Nuovo eruption (Phlegrean Fields, Italy): the role of syn-eruptive crystallization. *Bull. Volcanol.*, **67**, 601-621.
- Druitt, T.H. & Kokelaar, B.P. (2002): The eruption of Soufrière Hills Volcano, Montserrat, from 1995 to 1999. *Geol. Soc. London Mem.*, **21**, 639 p.
- Formenti, Y., Druitt, T.H., Kelfoun, K. (2003): Characterisation of the 1997, Vulcanian explosions of Soufrière Hills Volcano, Montserrat, by video analysis. *Bull. Volcanol.*, **65**, 587-605.
- Hammer, J.E., Cashman, K.V., Hoblitt, R., Newman, S. (1999): Degassing and microlite crystallization during the pre-climatic events of the 1991 eruption of the Mt. Pinatubo, Philippines. *Bull. Volcanol.*, **60**, 355-380.
- Jaupart, C. (1998): Gas loss from magmas through conduit walls during eruption. In: "The physics of explosive volcanic eruptions", J.S. Gilbert & R.S.J. Sparks, eds. *Geol. Soc. Spec. Publ.*, **145**, 73-90.
- Mastrolorenzo, G. & Pappalardo, L. (2006): Magma degassing and crystallization processes during eruptions of high-risk Neapolitan-volcanoes: evidence of common equilibrium rising processes in alkaline magmas. *Earth Planet. Sci. Letters*, **250**, 164-181.
- Polacci, M., Papale, P., Rosi, M. (2001): Textural heterogeneities in pumices from the climatic eruption of Mount Pinatubo, 15 June 1991, and implications for magma ascent dynamics. *Bull. Volcanol.*, **63**, 83-97.
- Polacci, M., Pioli, L., Rosi, M. (2003): The Plinian phase of the Campanian Ignimbrite eruption (Phlegrean Fields, Italy): evidence from density measurements and textural characterization of pumice. *Bull. Volcanol.*, **65**, 418-432.
- Rust, A.C. & Cashman, K.V. (2007): Multiple origins of obsidian pyroclasts and implications for changes in the dynamics of the 1300 B.P. eruption of Newberry Volcano, USA. *Bull. Volcanol.*, **69**, 825-845.
- Sparks, R.S.J., Barclay, J., Jaupart, C., Mader, H.M., Phillips, J.C. (1994): Physical aspects of magmatic degassing. I. Experimental and theoretical constraints on vesiculations. In: "Volatile in magmas", M.R. Carroll & J.R. Holloway, eds. *Rev. Mineral.*, **30**, 413-445.
- Stix, J., Torres, R.C., Narvaez, L.M., Cortes, J.G.P., Raigosa, A.J., Gomez, D.M., Castonguay, R. (1997): A model of vulcanian eruptions at Galeras volcano, Colombia. *J. Volcanol. Geotherm. Res.*, **77**, 285-303.
- Wohletz, K.H. (1983): Mechanisms of hydrovolcanic pyroclast formation: Grainsize, scanning electron microscopy, and experimental studies. *J. Volcanol. Geotherm. Res.*, **17**, 31-64.
- Wohletz, K., Orsi, G., De Vita, S. (1995): Eruptive mechanisms of the Neapolitan Yellow Tuff interpreted from stratigraphic, chemical and granulometric data. *J. Volcanol. Geotherm. Res.*, **67**, 263-290.
- Wright, H.M., Cashman, K.V., Rosi, M., Cioni, R. (2007): Breadcrust bombs as indicators of Vulcanian eruption dynamics at Guagua Pichincha volcano, Ecuador. *Bull. Volcanol.*, **69**, 281-300.